

How Alaska's Barry Arm Can Help Us Prepare for Climate Change Hazards

Bretwood Higman¹, Chad Briggs², Jeffrey Coe³, Chunli Dai⁴, Anja Dufresne⁵, Jeffrey Freymueller⁶, Marten Geertsema⁷, Peter Haeussler⁸, Mylene Fabienne Jacquemart⁹, Michele Koppes¹⁰, Anna Liljedahl¹¹, Patrick Lynett¹², Dmitry Nicolsky¹³, Lauren Schaefer¹⁴, Melissa Ward Jones¹¹, Robert Weiss¹⁵, Michael West¹⁶, and Gabriel Wolken¹³

¹Organization Not Listed

²University of Alaska Anchorage

³US Geological Survey

⁴Ohio State University Main Campus

⁵RWTH-Aachen University

⁶Michigan State University

⁷FLNRO

⁸USGS

⁹WSL Institute for Snow and Avalanche Research SLF

¹⁰University of British Columbia

¹¹Woods Hole Research Center

¹²University of Southern California

¹³University of Alaska Fairbanks

¹⁴USGS Geologic Hazards Science Center

¹⁵Virginia Tech

¹⁶Univ Alaska Fairbanks

November 23, 2022

Abstract

A slope at Barry Arm, in Alaska's Prince William Sound, is deforming at a varying rate up to tens of meters per year above a retreating glacier and deep fjord that is a popular recreational destination. If the estimated 500 million cubic meters of unstable material on this slope were to fail catastrophically, the impact of the landslide with the ocean would produce a tsunami that would not only endanger those in its immediate vicinity, but likely also those in more distant areas such as the port of Whittier, 50 km away. The discovery of this threat was happenstance, and the response so far has been cobbled together from over a dozen existing grants and programs. Remotely sensed imagery could have revealed this hazard a decade ago, but nobody was looking, highlighting our lack of coordination and preparedness for this growing hazard driven by climate change. As glaciers retreat, they can simultaneously destabilize mountain slopes and expose deep waters below, creating the potential for destructive tsunamis. The settings where this risk might occur are easily identified, but more difficult to assess and monitor. Unlike for volcanoes, active faults, landslides, and tectonic tsunamis, the US has conducted no systematic assessment of tsunamis generated by subaerial landslides, nor has the US established methods for monitoring or issuing warnings for such tsunamis. The U.S. National Tsunami Warning Center relies on seismic signals and sea-level measurements to issue warnings; however, landslides are more difficult to detect than earthquakes, and the resultant tsunamis often would reach vulnerable populations and infrastructure before water level gages could help estimate the magnitude of the tsunami. Also, integrating precursory

motion and other clues of an impending slope failure into a tsunami warning system has only been done outside the US (e.g. Norway: Blikra et al., 2012). Barry Arm is a dramatic case study highlighting these challenges and may provide a model for mitigating the threat of tsunamis generated by subaerial landslides enabled by glacial retreat elsewhere.

How Alaska's Barry Arm Can Help Us Prepare for Climate Change Hazards

How Alaska's Barry Arm Can Help Us Prepare for Climate Change Hazards
 Bretwood Higman¹, Chad Briggs², Jeffrey Coe³, Chunli Dai⁴, Anja Dufresne⁵, Jeffery Freymueller⁶, Marten Geertsema⁷, Peter Haeussler³, Mylène Jacquemart⁸, Michele Koppes⁹, Anna Liljedahl¹⁰, Pat Lynett¹¹, Dmitry Nicolsky¹², Lauren Schaefer³, Melissa Ward Jones¹³, Robert Weiss¹⁴, Michael West¹⁴, Gabriel Wolken¹⁵

¹Ground Truth Alaska, ²University of Alaska (Anchorage), ³US Geologic Survey, ⁴The Ohio State University, ⁵RWTH-Aachen University, ⁶Michigan State University, ⁷Ministry of Forests, Lands, Natural Resource Operations and Rural Development, ⁸University of Colorado (Boulder), ⁹University of British Columbia, ¹⁰Woodwell Climate Research Center, ¹¹University of Southern California, ¹²University of Alaska (Fairbanks), ¹³Virginia Tech, ¹⁴Alaska Earthquake Center, ¹⁵University of Alaska (Fairbanks) and Alaska Dept. of Natural Resources.

Barry Arm instability: Overview

In the summer of 2021, local and Alaska Native residents were visiting Barry Arm as part of the active-recreatory program with Chugach National Forest. The incident that one of the slopes along the western side of the fjord (labeled unstable) took shape, unfolded a sliding in the hinterland. The incident triggered a massive landslide. After a camera mounted, images passed the information to Chad Dai, who added it to a list of sites that were remaining using remote-sensed data. In April of 2022 she analyzed the site, and found that a large section of the slope was moving as a coherent block (Dai et al., 2022). Further analysis suggested that the slope poses a significant hazard through much of southeastern Prince William Sound. A closer evaluation of scientific and agency activities has begun taking steps to monitor the slope and inform the public of the possible hazard. The story of this ongoing effort is described in this poster.

Case Studies in Alaska's most hazardous slopes

The discovery of the instabilities around Barry Arm was unprecedented, and prior to the summer of 2021 no attempt had been made to systematically assess similar hazards throughout Alaska. Nonetheless, through the instability that led to the 2021 Barry Arm landslide and recent (Higman et al., 2022) had been ongoing programs previously, it had been identified a potential source of massive landslides. After the 2021 landslide and tsunami at Chugach Lake (Peters & Collins, 2019) geologists recognized that similar failures were possible in the future. In 2022, systematic reconnaissance of the hazard is only beginning. The only substantial slope that has been widely studied and mapped for landslide-generated tsunami hazard assessment in Alaska is the instability above Tidal Inlet in Glacier Bay (e.g. Nicolsky et al., 2017). However this slope is not being actively monitored.

Over the summer, we conducted a preliminary review of available remote-sensed data (primarily high resolution satellite imagery) across southern Alaska to identify slopes with obvious signs of instability, especially where they are near bodies of water where catastrophic failures might generate a tsunami, and where they are near human settlements.

Landslide tsunami mitigation: Examples worldwide

Norway's Eidsvik incident in which landslides generated deadly tsunamis in Norway have driven development of a robust research program and requirements for monitoring and warning. Their standards for landslide warning at least 10 hours before a failure, and at least 10 hours before in the area where the tsunami is high enough that an evacuation is needed. They rely on extensive monitoring infrastructure in unstable masses. However, because Norway is tectonically quite stable they are able to focus almost exclusively on landslides that have clear precursory signs of impending failure.

The level of monitoring and warning systems here yet to be tested against a tsunami-generating landslide. However in late summer of 2021 an instability had been generally monitored called forming a landslide of "Little Sister" (Dai et al., 2022). The failure was successfully monitored and the town at risk was evacuated, however this massive 15-magnitude had been formed and extended over 5 years.

Moving forward with Barry Arm

In Fall, in the next months after the Barry Arm instability was first identified as a potential hazard, scientists, engineers, and agencies have taken a number of steps to mitigate the risk. Local law enforcement along the fjord near the stable communities, authorities have issued evacuation plans, and various other needed operations at wilderness values in the area of risk. Alaska's Department of Natural Resources has conducted repeat lidar surveys and the US Geological Survey is using 3D LiDAR to monitor the instability. NOAA's Sea, Lake, and Overland Surveys from Space (SLIOS) has collected data on the Barry Arm, and the National Tsunami Warning Center has several data for water level forecasts nearby in Port Wells. The Alaska Earthquake Center deployed accelerometers and other instruments on the landslide and on a long slope across the fjord. Plans continue to expand the data collection network to include seismometers and tide gauges, as well as intense interest from the media resulting in a coverage schedule in media like the "New York Times", the "Washington Post", and the "BBC".

Unmapped stable regions

Figure 1: 2022 location of 3D LiDAR data collection (shown in blue) and 3D LiDAR data collection (shown in red).

Figure 2: 2022 location of 3D LiDAR data collection (shown in blue) and 3D LiDAR data collection (shown in red).

Figure 3: 2022 location of 3D LiDAR data collection (shown in blue) and 3D LiDAR data collection (shown in red).

Figure 4: 2022 location of 3D LiDAR data collection (shown in blue) and 3D LiDAR data collection (shown in red).

Figure 5: 2022 location of 3D LiDAR data collection (shown in blue) and 3D LiDAR data collection (shown in red).

Figure 6: 2022 location of 3D LiDAR data collection (shown in blue) and 3D LiDAR data collection (shown in red).

Figure 7: 2022 location of 3D LiDAR data collection (shown in blue) and 3D LiDAR data collection (shown in red).

Figure 8: 2022 location of 3D LiDAR data collection (shown in blue) and 3D LiDAR data collection (shown in red).

Figure 9: 2022 location of 3D LiDAR data collection (shown in blue) and 3D LiDAR data collection (shown in red).

Figure 10: 2022 location of 3D LiDAR data collection (shown in blue) and 3D LiDAR data collection (shown in red).

Figure 11: 2022 location of 3D LiDAR data collection (shown in blue) and 3D LiDAR data collection (shown in red).

Figure 12: 2022 location of 3D LiDAR data collection (shown in blue) and 3D LiDAR data collection (shown in red).

Figure 13: 2022 location of 3D LiDAR data collection (shown in blue) and 3D LiDAR data collection (shown in red).

Figure 14: 2022 location of 3D LiDAR data collection (shown in blue) and 3D LiDAR data collection (shown in red).

Figure 15: 2022 location of 3D LiDAR data collection (shown in blue) and 3D LiDAR data collection (shown in red).

Figure 16: 2022 location of 3D LiDAR data collection (shown in blue) and 3D LiDAR data collection (shown in red).

Figure 17: 2022 location of 3D LiDAR data collection (shown in blue) and 3D LiDAR data collection (shown in red).

Figure 18: 2022 location of 3D LiDAR data collection (shown in blue) and 3D LiDAR data collection (shown in red).

Figure 19: 2022 location of 3D LiDAR data collection (shown in blue) and 3D LiDAR data collection (shown in red).

Figure 20: 2022 location of 3D LiDAR data collection (shown in blue) and 3D LiDAR data collection (shown in red).

Figure 21: 2022 location of 3D LiDAR data collection (shown in blue) and 3D LiDAR data collection (shown in red).

Figure 22: 2022 location of 3D LiDAR data collection (shown in blue) and 3D LiDAR data collection (shown in red).

Figure 23: 2022 location of 3D LiDAR data collection (shown in blue) and 3D LiDAR data collection (shown in red).

Figure 24: 2022 location of 3D LiDAR data collection (shown in blue) and 3D LiDAR data collection (shown in red).

Figure 25: 2022 location of 3D LiDAR data collection (shown in blue) and 3D LiDAR data collection (shown in red).

Figure 26: 2022 location of 3D LiDAR data collection (shown in blue) and 3D LiDAR data collection (shown in red).

Figure 27: 2022 location of 3D LiDAR data collection (shown in blue) and 3D LiDAR data collection (shown in red).

Figure 28: 2022 location of 3D LiDAR data collection (shown in blue) and 3D LiDAR data collection (shown in red).

Figure 29: 2022 location of 3D LiDAR data collection (shown in blue) and 3D LiDAR data collection (shown in red).

Figure 30: 2022 location of 3D LiDAR data collection (shown in blue) and 3D LiDAR data collection (shown in red).

Figure 31: 2022 location of 3D LiDAR data collection (shown in blue) and 3D LiDAR data collection (shown in red).

Figure 32: 2022 location of 3D LiDAR data collection (shown in blue) and 3D LiDAR data collection (shown in red).

Figure 33: 2022 location of 3D LiDAR data collection (shown in blue) and 3D LiDAR data collection (shown in red).

Figure 34: 2022 location of 3D LiDAR data collection (shown in blue) and 3D LiDAR data collection (shown in red).

Figure 35: 2022 location of 3D LiDAR data collection (shown in blue) and 3D LiDAR data collection (shown in red).

Figure 36: 2022 location of 3D LiDAR data collection (shown in blue) and 3D LiDAR data collection (shown in red).

Figure 37: 2022 location of 3D LiDAR data collection (shown in blue) and 3D LiDAR data collection (shown in red).

Figure 38: 2022 location of 3D LiDAR data collection (shown in blue) and 3D LiDAR data collection (shown in red).

Figure 39: 2022 location of 3D LiDAR data collection (shown in blue) and 3D LiDAR data collection (shown in red).

Figure 40: 2022 location of 3D LiDAR data collection (shown in blue) and 3D LiDAR data collection (shown in red).

Figure 41: 2022 location of 3D LiDAR data collection (shown in blue) and 3D LiDAR data collection (shown in red).

Figure 42: 2022 location of 3D LiDAR data collection (shown in blue) and 3D LiDAR data collection (shown in red).

Figure 43: 2022 location of 3D LiDAR data collection (shown in blue) and 3D LiDAR data collection (shown in red).

Figure 44: 2022 location of 3D LiDAR data collection (shown in blue) and 3D LiDAR data collection (shown in red).

Figure 45: 2022 location of 3D LiDAR data collection (shown in blue) and 3D LiDAR data collection (shown in red).

Figure 46: 2022 location of 3D LiDAR data collection (shown in blue) and 3D LiDAR data collection (shown in red).

Figure 47: 2022 location of 3D LiDAR data collection (shown in blue) and 3D LiDAR data collection (shown in red).

Figure 48: 2022 location of 3D LiDAR data collection (shown in blue) and 3D LiDAR data collection (shown in red).

Figure 49: 2022 location of 3D LiDAR data collection (shown in blue) and 3D LiDAR data collection (shown in red).

Figure 50: 2022 location of 3D LiDAR data collection (shown in blue) and 3D LiDAR data collection (shown in red).

Figure 51: 2022 location of 3D LiDAR data collection (shown in blue) and 3D LiDAR data collection (shown in red).

Figure 52: 2022 location of 3D LiDAR data collection (shown in blue) and 3D LiDAR data collection (shown in red).

Figure 53: 2022 location of 3D LiDAR data collection (shown in blue) and 3D LiDAR data collection (shown in red).

Figure 54: 2022 location of 3D LiDAR data collection (shown in blue) and 3D LiDAR data collection (shown in red).

Figure 55: 2022 location of 3D LiDAR data collection (shown in blue) and 3D LiDAR data collection (shown in red).

Figure 56: 2022 location of 3D LiDAR data collection (shown in blue) and 3D LiDAR data collection (shown in red).

Figure 57: 2022 location of 3D LiDAR data collection (shown in blue) and 3D LiDAR data collection (shown in red).

Figure 58: 2022 location of 3D LiDAR data collection (shown in blue) and 3D LiDAR data collection (shown in red).

Figure 59: 2022 location of 3D LiDAR data collection (shown in blue) and 3D LiDAR data collection (shown in red).

Figure 60: 2022 location of 3D LiDAR data collection (shown in blue) and 3D LiDAR data collection (shown in red).

Figure 61: 2022 location of 3D LiDAR data collection (shown in blue) and 3D LiDAR data collection (shown in red).

Figure 62: 2022 location of 3D LiDAR data collection (shown in blue) and 3D LiDAR data collection (shown in red).

Figure 63: 2022 location of 3D LiDAR data collection (shown in blue) and 3D LiDAR data collection (shown in red).

Figure 64: 2022 location of 3D LiDAR data collection (shown in blue) and 3D LiDAR data collection (shown in red).

Figure 65: 2022 location of 3D LiDAR data collection (shown in blue) and 3D LiDAR data collection (shown in red).

Figure 66: 2022 location of 3D LiDAR data collection (shown in blue) and 3D LiDAR data collection (shown in red).

Figure 67: 2022 location of 3D LiDAR data collection (shown in blue) and 3D LiDAR data collection (shown in red).

Figure 68: 2022 location of 3D LiDAR data collection (shown in blue) and 3D LiDAR data collection (shown in red).

Figure 69: 2022 location of 3D LiDAR data collection (shown in blue) and 3D LiDAR data collection (shown in red).

Figure 70: 2022 location of 3D LiDAR data collection (shown in blue) and 3D LiDAR data collection (shown in red).

Figure 71: 2022 location of 3D LiDAR data collection (shown in blue) and 3D LiDAR data collection (shown in red).

Figure 72: 2022 location of 3D LiDAR data collection (shown in blue) and 3D LiDAR data collection (shown in red).

Figure 73: 2022 location of 3D LiDAR data collection (shown in blue) and 3D LiDAR data collection (shown in red).

Figure 74: 2022 location of 3D LiDAR data collection (shown in blue) and 3D LiDAR data collection (shown in red).

Figure 75: 2022 location of 3D LiDAR data collection (shown in blue) and 3D LiDAR data collection (shown in red).

Figure 76: 2022 location of 3D LiDAR data collection (shown in blue) and 3D LiDAR data collection (shown in red).

Figure 77: 2022 location of 3D LiDAR data collection (shown in blue) and 3D LiDAR data collection (shown in red).

Figure 78: 2022 location of 3D LiDAR data collection (shown in blue) and 3D LiDAR data collection (shown in red).

Figure 79: 2022 location of 3D LiDAR data collection (shown in blue) and 3D LiDAR data collection (shown in red).

Figure 80: 2022 location of 3D LiDAR data collection (shown in blue) and 3D LiDAR data collection (shown in red).

Figure 81: 2022 location of 3D LiDAR data collection (shown in blue) and 3D LiDAR data collection (shown in red).

Figure 82: 2022 location of 3D LiDAR data collection (shown in blue) and 3D LiDAR data collection (shown in red).

Figure 83: 2022 location of 3D LiDAR data collection (shown in blue) and 3D LiDAR data collection (shown in red).

Figure 84: 2022 location of 3D LiDAR data collection (shown in blue) and 3D LiDAR data collection (shown in red).

Figure 85: 2022 location of 3D LiDAR data collection (shown in blue) and 3D LiDAR data collection (shown in red).

Figure 86: 2022 location of 3D LiDAR data collection (shown in blue) and 3D LiDAR data collection (shown in red).

Figure 87: 2022 location of 3D LiDAR data collection (shown in blue) and 3D LiDAR data collection (shown in red).

Figure 88: 2022 location of 3D LiDAR data collection (shown in blue) and 3D LiDAR data collection (shown in red).

Figure 89: 2022 location of 3D LiDAR data collection (shown in blue) and 3D LiDAR data collection (shown in red).

Figure 90: 2022 location of 3D LiDAR data collection (shown in blue) and 3D LiDAR data collection (shown in red).

Figure 91: 2022 location of 3D LiDAR data collection (shown in blue) and 3D LiDAR data collection (shown in red).

Figure 92: 2022 location of 3D LiDAR data collection (shown in blue) and 3D LiDAR data collection (shown in red).

Figure 93: 2022 location of 3D LiDAR data collection (shown in blue) and 3D LiDAR data collection (shown in red).

Figure 94: 2022 location of 3D LiDAR data collection (shown in blue) and 3D LiDAR data collection (shown in red).

Figure 95: 2022 location of 3D LiDAR data collection (shown in blue) and 3D LiDAR data collection (shown in red).

Figure 96: 2022 location of 3D LiDAR data collection (shown in blue) and 3D LiDAR data collection (shown in red).

Figure 97: 2022 location of 3D LiDAR data collection (shown in blue) and 3D LiDAR data collection (shown in red).

Figure 98: 2022 location of 3D LiDAR data collection (shown in blue) and 3D LiDAR data collection (shown in red).

Figure 99: 2022 location of 3D LiDAR data collection (shown in blue) and 3D LiDAR data collection (shown in red).

Figure 100: 2022 location of 3D LiDAR data collection (shown in blue) and 3D LiDAR data collection (shown in red).

Bretwood Higman¹, Chad Briggs², Jeffrey Coe³, Chunli Dai⁴, Anja Dufresne⁵, Jeffery Freymueller⁶, Marten Geertsema⁷, Peter Haeussler³, Mylène Jacquemart⁸, Michele Koppes⁹, Anna Liljedahl¹⁰, Pat Lynett¹¹, Dmitry Nicolsky¹², Lauren Schaefer³, Melissa Ward Jones¹⁰, Robert Weiss¹³, Michael West¹⁴, Gabriel Wolken¹⁵

¹Ground Truth Alaska, ²University of Alaska (Anchorage), ³US Geologic Survey, ⁴The Ohio State University, ⁵RWTH-Aachen University, ⁶Michigan State University, ⁷Ministry of Forests, Lands, Natural Resource Operations and Rural Development, ⁸University of Colorado (Boulder), ⁹University of British Columbia, ¹⁰Woodwell Climate Research Center, ¹¹University of Southern California, ¹²University of Alaska (Fairbanks), ¹³Virginia Tech, ¹⁴Alaska Earthquake Center, ¹⁵University of Alaska (Fairbanks) and Alaska Dept. of Natural Resources.

PRESENTED AT:



BARRY ARM INSTABILITY: OVERVIEW

In the summer of 2019, local artist Valisa Higman was visiting Barry Arm as part of her artist-in-residency program with Chugach National Forest. She noticed that one of the slopes along the western side of the fjord looked unstable, took a photo, and passed it along to her brother Bretwood Higman, who studies tsunami hazards. After a cursory assessment, Higman passed the information to Chunli Dai, who added it to a list of sites she was examining using remote-sensed data. In April of 2020 she analyzed the site, and found that a large section of the slope was moving as a coherent block (Dai et al., 2020 (<https://agupubs.onlinelibrary.wiley.com/doi/abs/10.1029/2020GL089800>)). Further analysis suggested that the slope poses a significant hazard through much of northwestern Prince William Sound. A loose collaboration of academic and agency scientists has begun taking steps to monitor the slope and inform the public of the possible hazard. The story of this ongoing effort is the subject of this poster.

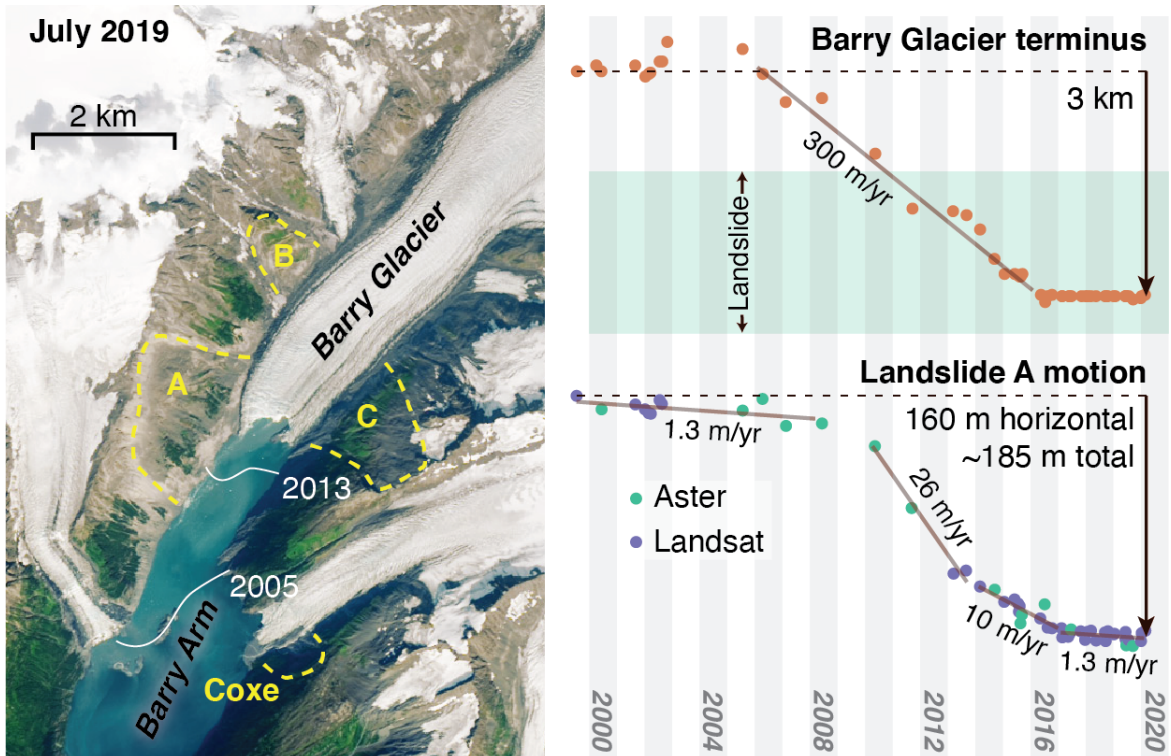


Figure 1. Instability "A" was the subject of the initial analysis, but further study identified additional instabilities. Barry Arm instability "A" experienced a spurt of motion between 2009 and 2016, corresponding to a period of rapid retreat of Barry Glacier.

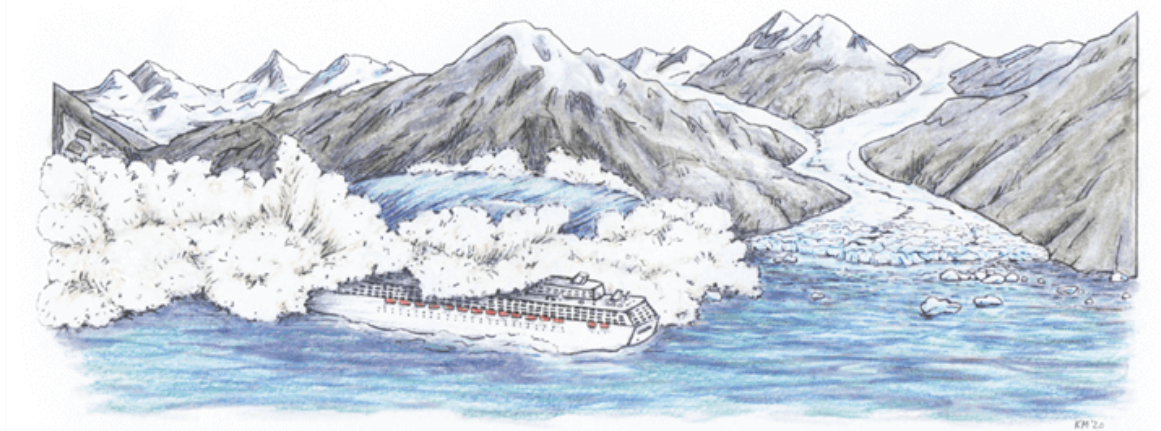
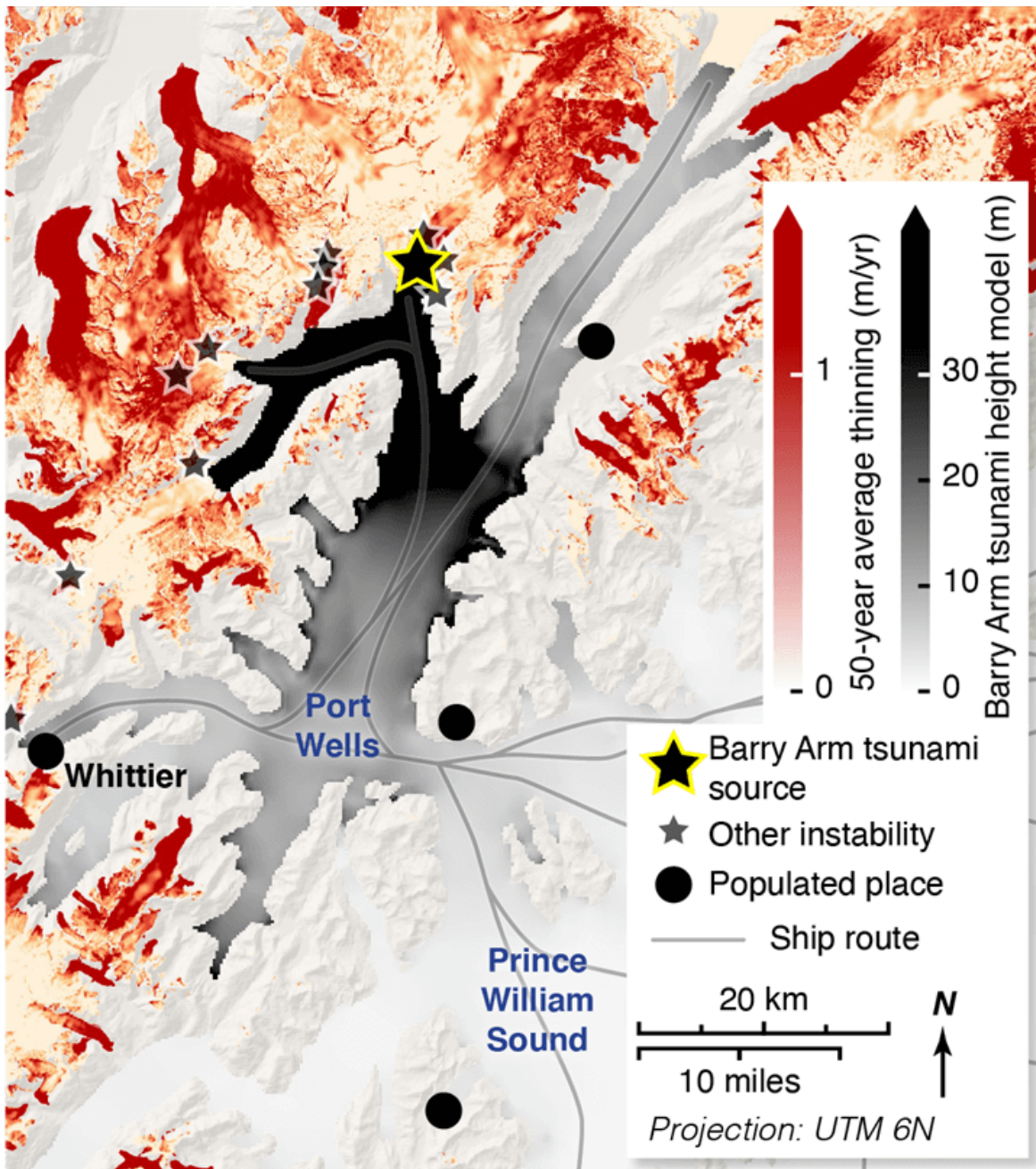
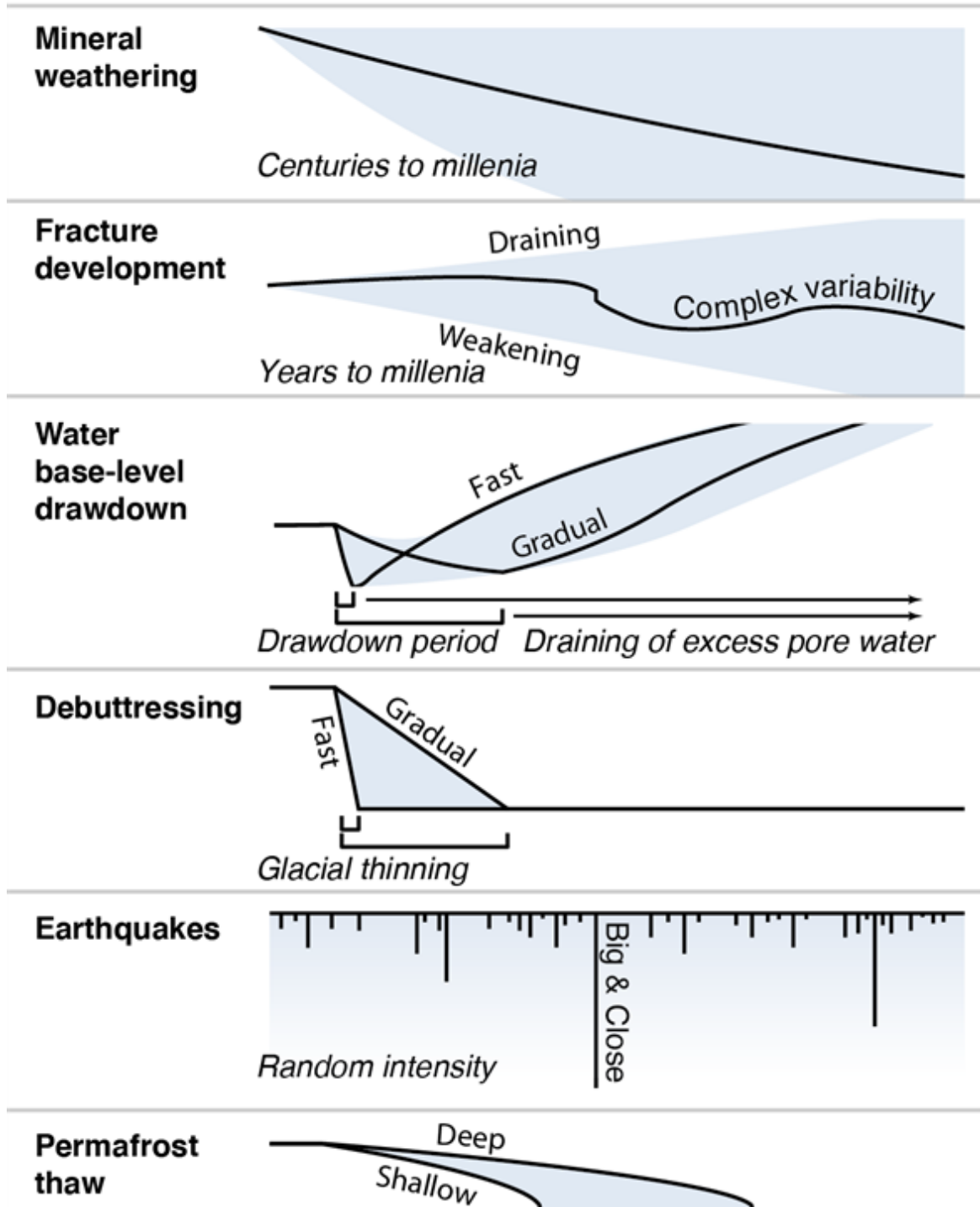
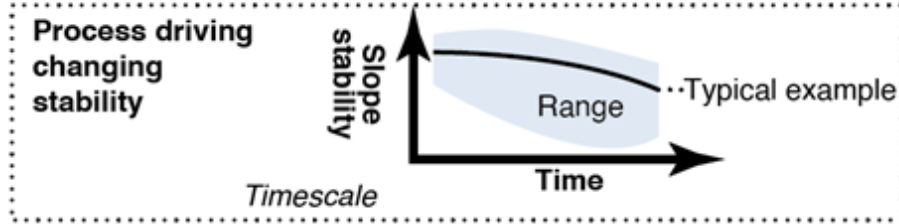


Figure 2. The emerging hazard at Barry Arm is plausibly linked to the retreat of Barry Glacier. Preliminary modeling of the tsunami that might be generated if Barry Arm instability A failed catastrophically, shows that it could impact not only the immediate vicinity of the landslide but also more distant areas of Port Wells, and could focus at the heads of bays - notably near the town of Whittier 50 km away. Whittier and Port Wells are popular cruise ship destinations, regularly bringing thousands of passengers and crew into areas of potential landslide-generated tsunami danger.

Barry Arm is an example of a climate-driven hazard. Historically, large landslide-generated tsunamis have been fairly infrequent - four have generated runup over 50 m in Alaska in the past 100 years. However, multiple climate change-related factors may be increasing the risk of these events, including debuttressing as glaciers retreat, mountain weakening as alpine permafrost warms and thaws, and increased pore-fluid pressure during increasingly large precipitation and snowmelt events.

Layout for each panel below:



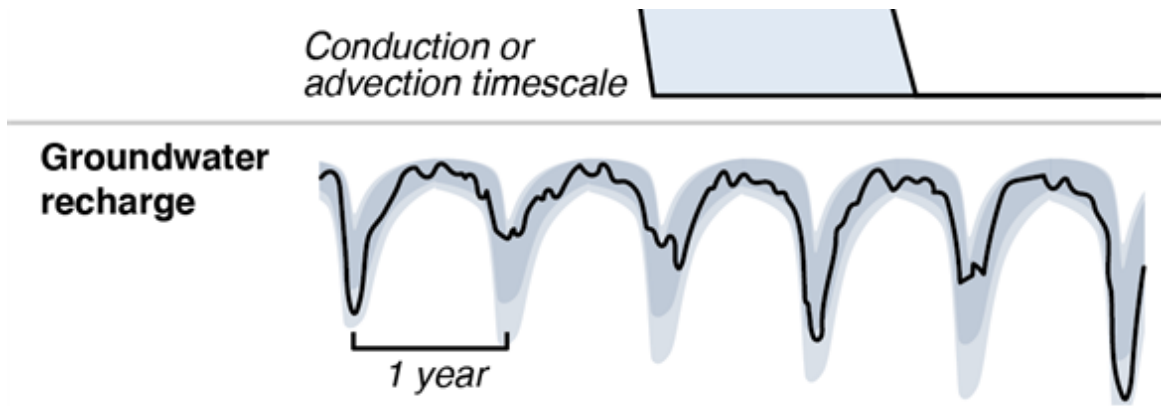


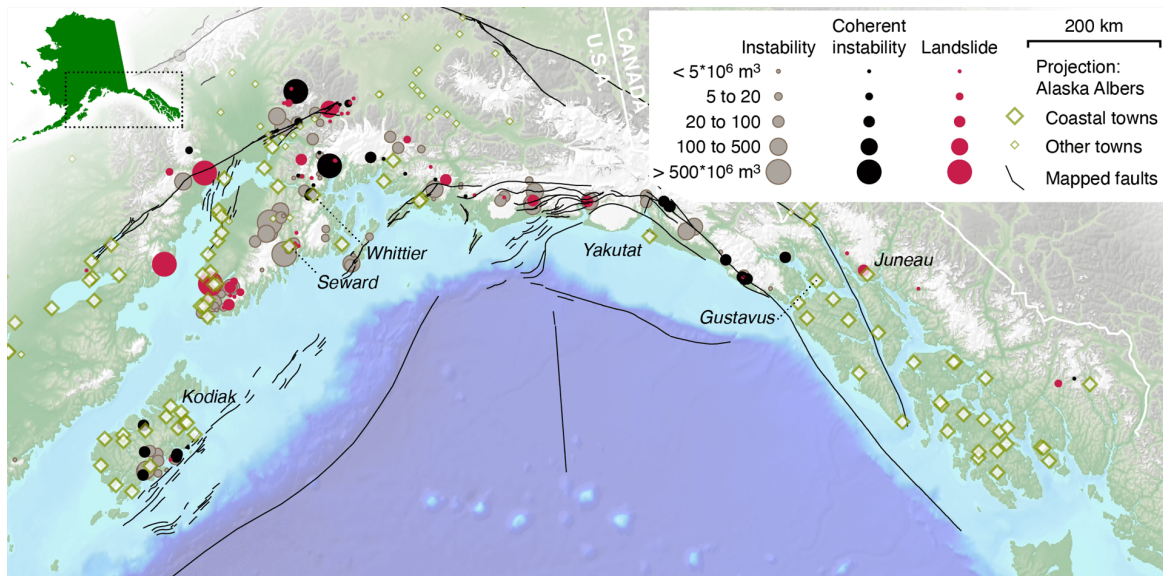
Figure 3: Qualitative illustration of multiple factors that change the stability of a slope over time.

At Barry Arm specifically, it's likely that water base-level drawdown, debuttreasing, and groundwater recharge are some of the biggest factors in play - all processes that are acting here on the timescale of years to days. Even if these dynamics wouldn't lead to catastrophic failure by themselves, they may prime the slope for failure during an earthquake. In the coming century, it is likely that this slope will experience further debuttreasing and consequent water base-level drawdown, more intense rainfall than it has in the past, and violent earthquake shaking.

CASE STUDIES IN ALASKA'S MOST HAZARDOUS SLOPES

The discovery of the instabilities around Barry Arm was happenstance, and prior to the summer of 2020 no attempt had been made to systematically assess similar hazards throughout Alaska. Similarly, though the instability that led to the 2015 Taan landslide and tsunami (Higman et al., 2018 (<https://www.nature.com/articles/s41598-018-30475-w>)) had been mapped by geologists previously, it hadn't been identified as a potential source of tsunami hazard. After the 1967 landslide and tsunami at Grewingk Lake (Wiles & Calkin, 1992 (<https://pubs.geoscienceworld.org/gsa/gsabulletin/article-abstract/106/2/281/182922/Late-Holocene-high-resolution-glacial-chronologies?redirectedFrom=fulltext>)) geologists recognized that similar failures were possible in the future. As of 2020, systematic evaluation of this hazard is only beginning. The only subaerial slope that has been widely studied and incorporated into landslide-generated tsunami hazard assessments in Alaska is the instability above Tidal Inlet in Glacier Bay (e.g. Wieczorek et al. 2007 (https://www.uas.alaska.edu/arts_sciences/naturalsciences/envs/faculty_staff/pubs/Tidal_Inlet_landslide.pdf)). However this slope is not being actively monitored.

Over the summer, we conducted a preliminary review of available remote-sensed data (primarily high resolution satellite imagery) across southern Alaska to identify slopes with obvious signs of instability, especially where they are near bodies of water where catastrophic failure might generate a tsunami, and where they are near human vulnerabilities.



Our preliminary map of large instabilities and landslides in Alaska. We made the distinction between a generic "Instability" - any sign of ground deformation, and a "Coherent instability" where a defined basal failure plane can be discerned. Most of these would fit the typical definition of deep-seated gravitational slope deformation (e.g. Dramis and Valvo, 1994 (<https://www.sciencedirect.com/science/article/abs/pii/001379529490040X>)).

This effort is only in its most preliminary stage, but a number of sites have risen to the top (in addition to Grewingk Glacier Lake and Tidal Inlet, which were previously known). We are in the process of reaching out to potentially affected communities, and attempting to advance our understanding of these sites:

Portage Glacier: The proglacial lake below Portage Glacier is a popular recreational and tourist destination, with a visitor center, parking lots, a highway, and a tour boat operation in and near the lake. A volume of around 5 Mm^3 above the glacier is heavily fractured and actively deforming.

Turner Glacier: A broad slope with numerous anticarps and tension cracks sits above Turner Glacier, not far from the terminus of Hubbard Glacier. The unstable mass is likely tens of millions of cubic meters, and recent geologic fieldwork in the area found active sink holes along one of the scarps. The waters directly below it are a popular summer cruise ship destination. A tsunami here might have an impact in the nearby town of Yakutat as well.

Maynard Mountain: A rotational slump with a volume of a few tens of millions of cubic meters and several concentric normal scarps on a slope laced with anticarps. The slope shows no clear signs of deformation in the past few decades based on high-res aerial and satellite imagery, however if it were to fail it could generate a tsunami in Passage Canal just a kilometer from the community of Whittier.

Mount Marathon: This is one of the most climbed mountains in Alaska, rising above the city of Seward. The south side of the mountain has cracks and scarps that suggest a mass that may be over 100 Mm³ that has slipped in the past. Active scree slopes in the area may suggest geologically recent deformation. A large failure here could flow directly through downtown Seward across its waterfront into Resurrection Bay. In addition to direct landslide and tsunami threat from a large landslide, a small failure of this slope could create a landslide dam that could fail catastrophically and flood downtown Seward.

Columbia Glacier: Columbia Glacier has experienced extraordinary retreat in the past several decades. A slope near the current terminus of the glacier is laced with fractures and scarps. It has experienced 100s of meters of debuttressing in the past few decades, and will likely be completely debuttressed within a decade. The volume (10s of millions of cubic meters) of material here is sufficient to generate a large tsunami that would have severe impacts throughout the newly deglaciated fjord, which is a popular tourist destination. It might have impacts to further areas as well.

Sitkalidak Strait: Along the outer coast of Kodiak Island, many slopes show signs of deep-seated deformation. Of particular concern are several instabilities along Sitkalidak Strait - a deep confined water body with the town of Old Harbor along its shore. These areas are separated from the modern cryosphere, so are not experiencing strong changes related to debuttressing or permafrost melt, but increased precipitation could still impact these slopes.

Kodiak Coast Guard Base: The Coast Guard operates a major base near the city of Kodiak, and on the slope above the harbor is an arcuate scarp defining a rotational slump. The toe of this slump may have been weakened by road construction activities, raising the possibility of a tsunamigenic landslide within the port itself.

LANDSLIDE TSUNAMI MITIGATION: EXAMPLES WORLDWIDE

Norway: Historic incidents in which landslides generated deadly tsunamis in Norway have driven development of a robust research program and requirements for monitoring and warning. Their standards seek to provide warning at least 72 hours before a failure, and at least 12 hours before in the case where the certainty is high enough that an evacuation is ordered. They rely on extensive monitoring instrumentation in unstable masses. However, because Norway is tectonically quite stable they are able to focus almost exclusively on landslides that have clear precursory signs of impending failure.

The installed monitoring and warning systems have yet to be tested against a tsunami-generating landslide, however in late summer of 2019 an instability that had been aggressively monitored failed forming a landslide off "Little Man" mountain in Norway (<https://www.nytimes.com/2019/09/07/world/europe/norway-mountain-little-man.html>). The failure was successfully anticipated and the town at risk was evacuated, however this was after 15 warnings had been issued and canceled over 5 years.

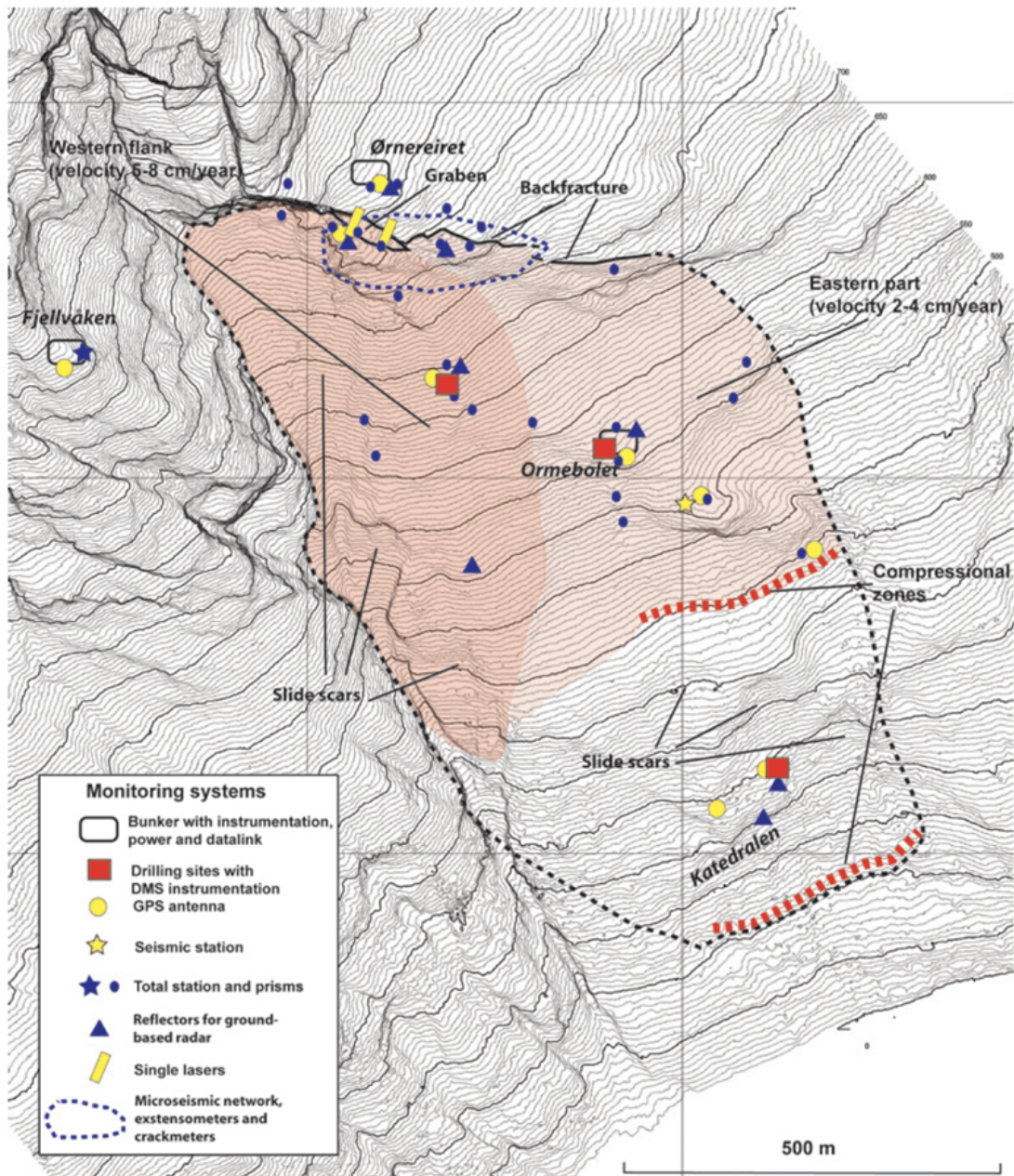


Fig. 3 The Åknes rockslide with the main scenarios in different colors, geomorphological features and the instrumentation (modified from BLIKRA, 2012)

Figure 5: Example of monitoring for an instability in Norway.

Greenland: Greenland has a history of large landslide-generated tsunamis, including in 2000 and 2017. The 2017 Karrat Fjord tsunami largely destroyed the village of Nuugaatsiaq, killing four people. Given the likelihood other nearby slopes might fail, Nuugaatsiaq and one other village were evacuated, and remain abandoned today. In collaboration with the government of Denmark, Greenlandic scientists are working to better understand landslide risk throughout Greenland.

[VIDEO] <https://www.youtube.com/embed/tWvYFMo2LsQ?rel=0&fs=1&modestbranding=1&rel=0&showinfo=0>

Figure 6: Eyewitness video of the 2017 Karrat Fjord tsunami impacting Nuugaatsiaq.

Indonesia: Though cryosphere change isn't a major landslide driver in Indonesia, several landslide-generated tsunamis in recent years have motivated development of active landslide monitoring. Anak Krakatau in Sunda Strait generated a tsunami during an eruption in 2018 that killed over 400 people. The degree to which the eruption itself and consequent landsliding contributed to the tsunami is still under investigation, but it is clear that a large landslide did occur (Ye et al., 2020 (<https://advances.sciencemag.org/content/advances/6/3/eaaz1377.full.pdf>)). Indonesian scientists hope to deploy instrumentation including continuous GPS and water level gages to provide the basis for warnings in this area. The challenges in this context parallel those faced in Alaska and elsewhere where climate driven change is leading to emerging tsunami risk mitigation needs.



Figure 7: Damage from the 22 Dec 2018 Sunda Strait Tsunami

MOVING FORWARD WITH BARRY ARM

So Far: In the eight months since the Barry Arm instability was first identified as a serious hazard, stakeholders, scientists, and agencies have taken a number of steps to mitigate the risk. Local tour operators have changed the routes they take customers on, adventurers have shifted kayaking plans, and visitors have canceled reservations at wilderness cabins in the area of risk. Alaska's Department of Natural Resources has conducted repeat lidar surveys and the US Geological Survey is using InSAR to monitor ongoing deformation (<https://www.sciencebase.gov/catalog/item/5efa15fd82ced62aaee1c7c>). NOAA has collected new bathymetry, and the National Tsunami Warning Center has scouted sites for water level sensors nearby in Port Wells. The Alaska Earthquake Center deployed seismometers and other instruments on the landslide and on a facing slope across the fjord. News continues to spread, thanks to active outreach from involved scientists and stakeholders, as well as intense interest from the media resulting in coverage worldwide in outlets like the New York Times (<https://www.nytimes.com/2020/05/14/climate/alaska-landslide-tsunami.html>), the Guardian (<https://www.theguardian.com/environment/2020/oct/18/alaska-climate-change-tsunamis-melting-permafrost>), NASA (<https://earthobservatory.nasa.gov/images/147345/the-specter-of-a-mega-tsunami-in-alaska>), and the Atlantic (<https://www.theatlantic.com/science/archive/2020/11/alaskas-tsunami-time-bomb/617082/>).

Unwrapped interferogram

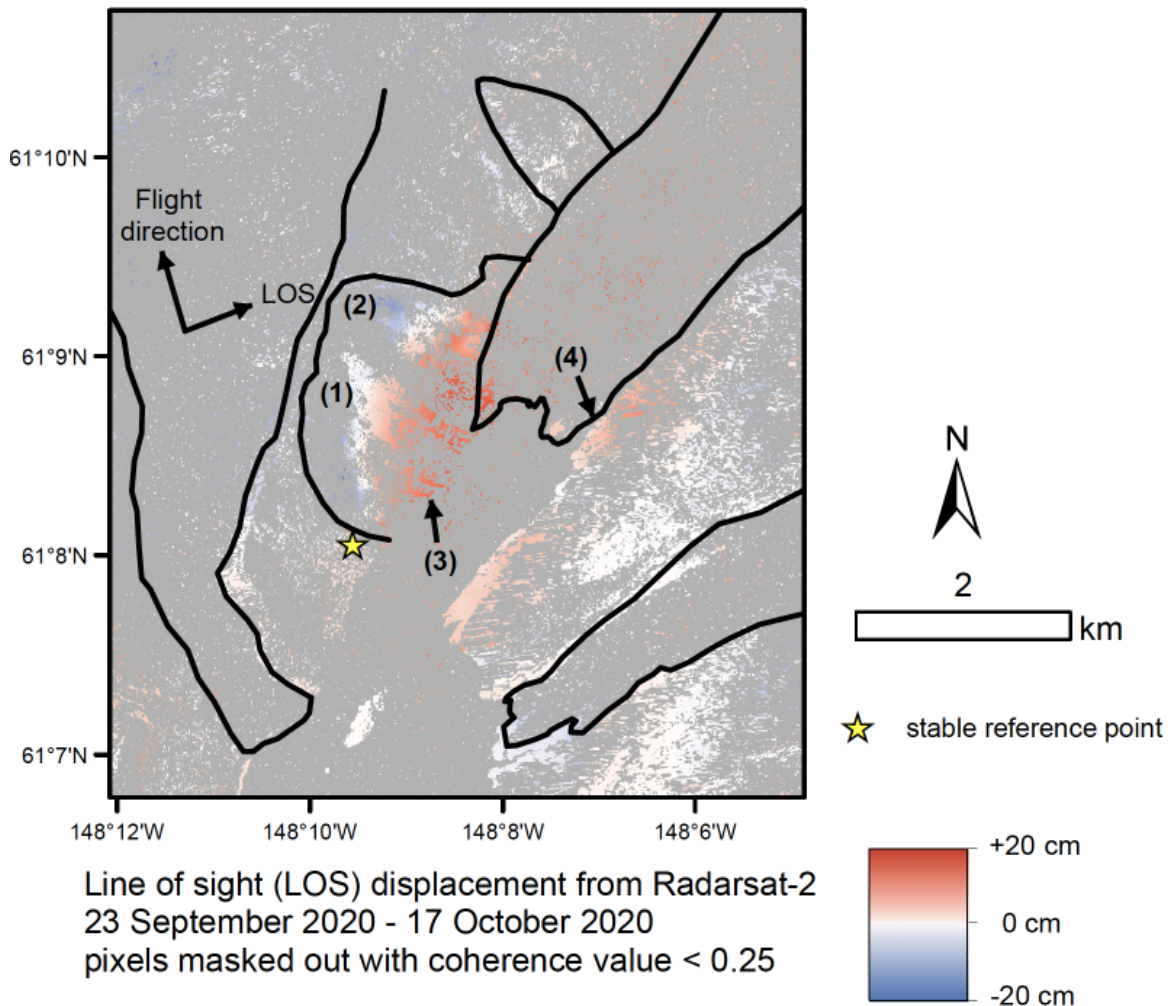


Figure 8: USGS analysis of InSAR (<https://www.sciencebase.gov/catalog/item/5efa15fd82ced62aaee1c7c>) deformation mapping in late Sept. and early Oct. The deformation is line of sight, and shows negative deformation up high and positive deformation down low - consistent with rotational motion of the whole slide mass. Note (4) points to an area on the opposite side of the glacier that may be deforming some as well. Details related to this analysis are further explored on another AGU poster (Daanen et al., 2020 (/Default.aspx?s=AE-2A-A1-EF-F1-0C-00-00-20-AE-5B-AB-62-BA-F2-8A)).

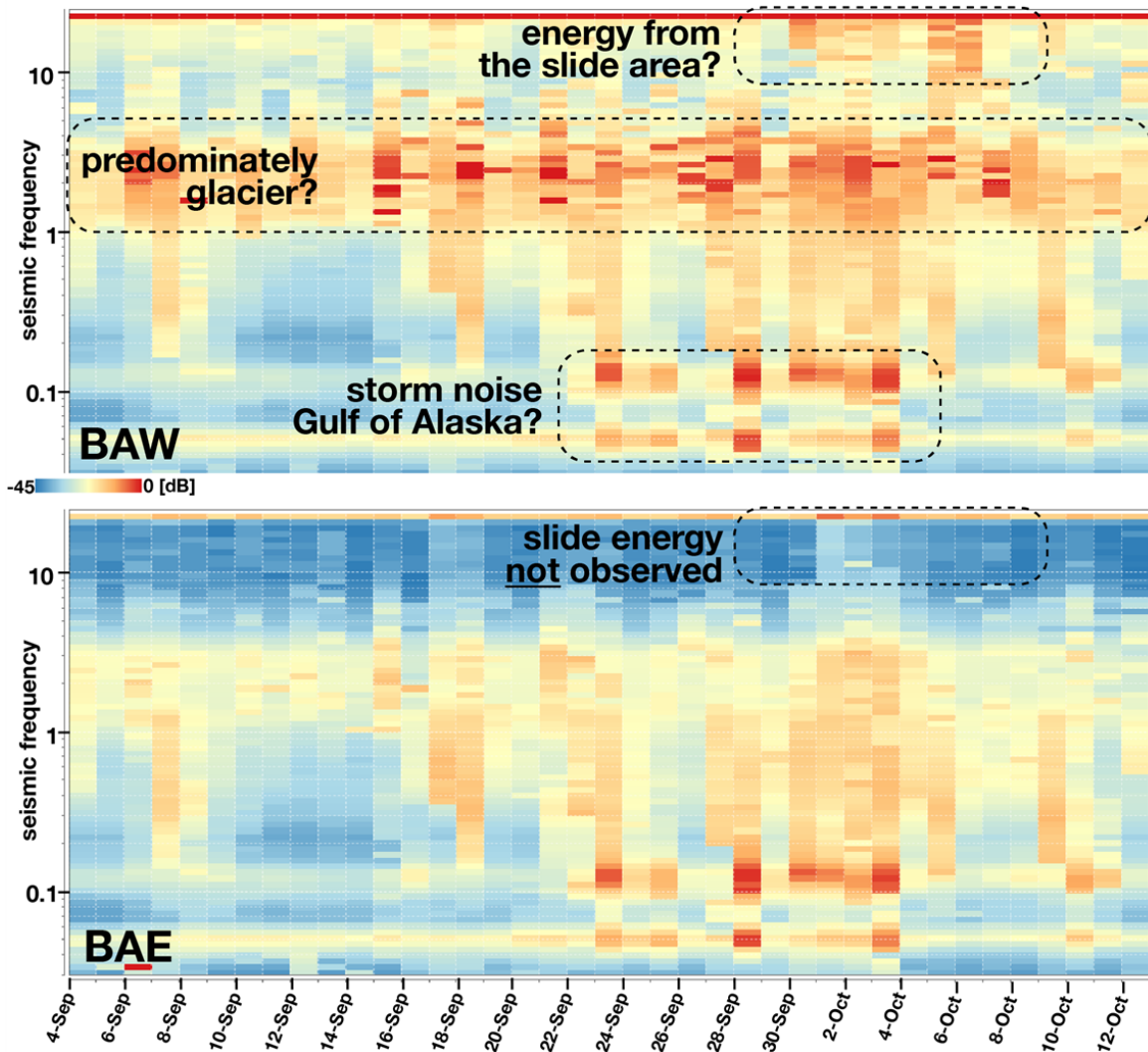


Figure 9: During the same time period where the deformation in Fig. 8 is documented, differences between seismic energy from two seismometers near Barry Arm show evidence of activity as well. BAW sits atop the unstable mass, while BAE is on a more stable mountain on the opposite side of the fjord. At the end of September a series of rainstorms hit the area, followed a few days later by high-frequency noise apparent only on the slide mass.

Next Steps: The National Tsunami Warning Center continues to work toward a fully functional tsunami warning system specific to the threat presented by Barry Arm. The deployment of telemetered water level gages will help bring this system fully online. DNR and collaborating researchers are also working to secure funding for a telemetered DGPS on the slide mass to monitor motion. A broad collaboration of academic scientists have submitted a proposal to NSF's Coastlines and People program for funding to study landslide-generated tsunami hazards across southern Alaska. If selected, this research would support extensive further research on Barry Arm, but would not support long-term monitoring.

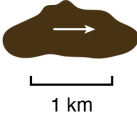
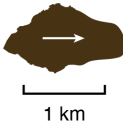
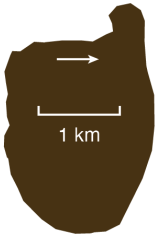
What does the future look like? Alaska and the US are still a long ways from the sort of systematic, policy-supported development of monitoring and warning that is employed in Norway. It will take a concerted effort involving local stakeholders, academics, and government agencies over years to decades to reach the point where the hazard presented by landslide-generated tsunamis throughout Alaska is well-understood, and has been mitigated to the extent that is practical.

However, Barry Arm is likely one of the most dangerous slopes in Alaska, and progress has been rapid, albeit haphazard, toward mitigating the risk. Hopefully, there will soon be improved instrumentation on the slide mass, and strong cooperation between agencies responsible for both understanding the monitoring system and issuing tsunami warnings.

ABSTRACT

A slope at Barry Arm, in Alaska's Prince William Sound, is deforming at a varying rate up to tens of meters per year above a retreating glacier and deep fjord that is a popular recreational destination. If the estimated 500 million cubic meters of unstable material on this slope were to fail catastrophically, the impact of the landslide with the ocean would produce a tsunami that would not only endanger those in its immediate vicinity, but likely also those in more distant areas such as the port of Whittier, 50 km away. The discovery of this threat was happenstance, and the response so far has been cobbled together from over a dozen existing grants and programs. Remotely sensed imagery could have revealed this hazard a decade ago, but nobody was looking, highlighting our lack of coordination and preparedness for this growing hazard driven by climate change. As glaciers retreat, they can simultaneously destabilize mountain slopes and expose deep waters below, creating the potential for destructive tsunamis. The settings where this risk might occur are easily identified, but more difficult to assess and monitor. Unlike for volcanoes, active faults, landslides, and tectonic tsunamis, the US has conducted no systematic assessment of tsunamis generated by subaerial landslides, nor has the US established methods for monitoring or issuing warnings for such tsunamis. The U.S. National Tsunami Warning Center relies on seismic signals and sea-level measurements to issue warnings; however, landslides are more difficult to detect than earthquakes, and the resultant tsunamis often would reach vulnerable populations and infrastructure before water level gages could help estimate the magnitude of the tsunami. Also, integrating precursory motion and other clues of an impending slope failure into a tsunami warning system has only been done outside the US (e.g Norway: Blikra et al., 2012). Barry Arm is a dramatic case study highlighting these challenges and may provide a model for mitigating the threat of tsunamis generated by subaerial landslides enabled by glacial retreat elsewhere.

The Barry Arm slope instability compared to Alaska's largest tsunami-generating landslides

Water Body	Lituya Bay	Grewingk Lake	Taan Fiord	Barry Arm
Landslide area (Arrow indicates downhill)				
Failure Year	1958	1967	2015	
Max tsunami runup	524 m	60 m	193 m	
Volume	30 million m ³	83 million m ³	60 million m ³	500 million m ³
Elevation (center of mass)	610 m	350 m	250 m	400 m
Slope	40°	33°	25°	36°
Energy (x10 ¹⁴ J)	4.6	7.4	3.8	51.0

(https://agu.confex.com/data/abstract/agu/fm20/0/1/Paper_718110_abstract_684759_0.png)